Available online at www.sciencedirect.com

ScienceDirect

IFAC Papers Online CONFERENCE PAPER ARCHIVE

IFAC-PapersOnLine 49-7 (2016) 1175–1180

A Multi-rate Moving Horizon Estimation Framework for Electric Arc Furnace Operation ⋆

Smriti Shyamal * **Christopher L.E. Swartz** *

* *Department of Chemical Engineering, McMaster University, 1280 Main St W, Hamilton ON L8S 4L7, Canada (e-mail: swartzc@mcmaster.ca).*

Abstract: Electric arc furnaces (EAFs) are widely used in steel industries to produce molten steel from scrap metal. EAF operation, being a highly energy intensive process, is characterized by a limited number of measurements at multiple rates, most of which do not correspond to system states. The ability to estimate the states would enhance the application of control and real-time optimization strategies. In this work, a multi-rate moving horizon estimation (MHE) framework for EAF operation under flat-bath conditions is introduced and implemented. Key features are the restructuring of the MHE problem to a parameter estimation problem, multi-rate measurement handling, and use of a nonlinear model. The approach is implemented in the `gPROMS` (General Process Modeling System) modeling language. The components of the framework are presented, and the method is applied to a case study illustrating its performance.

Keywords: State estimation, electric arc furnace, dynamic optimization, moving horizon estimation, multi-rate measurements.

1. INTRODUCTION

Electric arc furnaces (EAFs) are widely used for production of steel by melting scrap steel and adjusting its chemistry. This is a highly energy intensive, complex batch process involving both electrical and chemical energy to melt scrap. The electrical energy is transfered through electrodes, and burners are used to inject natural gas and oxygen, which provide chemical energy through combustion. The melting continues and a flat bath of molten steel is formed. The flat bath conditions usually last for the final 20 minutes of the batch duration. The oxygen reacts with metals to form oxides which become components of the slag layer floating on top of the molten steel. Slag chemistry is varied by direct addition of carbon, lime and dolomite through the roof of the furnace and by adjusting oxygen and carbon lancing. The high energy consumption motivates the development of estimation and control strategies for EAFs.

Due to the harsh operating conditions, EAFs lack measurements and most of the states are not directly measured. State knowledge is very important in real-time control applications. There are limited applications of state estimation for EAF operation. Billings et al. (1979) applied the extended Kalman filter (EKF) to the refining stage of EAF operation but the model had 4 states, which are insufficient to capture the detailed process dynamics. Wang et al. (2005) used an EKF to identify the arc current parameter for obtaining the electrical properties of the EAF load. However, the EAF model only involved the power system. Ghobara (2013) implemented a constrained multi-rate EKF to estimate the states of an EAF system using plant measurements. The EKF showed an acceptable performance in tracking the true states of the process, even in the presence of parametric plant-model mismatch. Of the many available tools for state estimation, moving horizon estimation (MHE) is gaining popularity (Allgöwer et al., 1999) due to the ability to handle constraints and to use computationally efficient numerical optimization algorithms. Although different versions of the Kalman filter such as the EKF, unscented Kalman filter etc. are employed by some researchers, many studies have shown MHE to have superior performance than Kalman filters (Lima and Rawlings, 2011).

The MHE problem consists of solving a nonlinear dynamic optimization problem subject to the nonlinear system under consideration and some other constraints specified by the user. It uses a finite set of past available measurements to reconstruct the full state of the process, thus keeping the optimization problem numerically tractable. The use of a finite size window of measurements by MHE provides a natural framework to include measurements with different sampling rates. López-Negrete and Biegler (2012) mention that including the slow measurements for state estimation can improve system observability. They proposed a variable structure multi-rate MHE and illustrated it using two simulation examples.

Direct techniques used for solving the dynamic optimization problem of MHE are sequential (i.e., single shooting), simultaneous (i.e., full transcription), and multiple-shooting methods. Simultaneous and multiple shooting methods have been extensively explored by researchers for MHE applications incorporating large scale differential-

⋆ This work is supported by the McMaster Steel Research Center (SRC) and the McMaster Advanced Control Consortium (MACC).

10.1016/j.ifacol.2016.07.365

algebraic equation (DAE) systems. The contributions are due to the developments and applications related to tools: AMPL (Fourer et al., 1990) with solver IPOPT (Zavala and Biegler, 2009), ACADO toolkit (Houska et al., 2011), JModelica.org (Åkesson et al., 2010) and MUSCOD II (Kraus et al., 2006). However, the sequential method has received less attention. Although gPROMS (Process Systems Enterprise Ltd., 2015) provides commercial products for model-based chemical engineering and has capabilities for solving dynamic optimization using shooting algorithms, it has not been clear whether MHE can be readily formulated within the gPROMS framework. It transpires that it is relatively straightforward to formulate MHE as a parameter estimation problem in gPROMS (Pantelides, 2015). This is intuitive as both MHE and parameter estimation have a similar approach to maximize a joint probability function, given the measurements. However, for MHE it is the joint probability for a trajectory of state values whereas in case of parameter estimation it is for the mathematical model predicting the measurement values.

In this paper, we develop a rigorous framework to do MHE for the EAF process. Multi-rate MHE is posed as a parameter estimation problem where the discrete process noise terms are handled using a continuous function. The formulation is particularly suitable for applications in sequential dynamic optimization platforms such as gPROMS/gEST. The reformulation is studied for a first-principles dynamic EAF model developed originally in MacRosty and Swartz (2005). The multi-rate MHE is utilized to estimate states for an EAF heat (batch) under flat bath conditions. The measurements used in estimating the states are assumed to have no delays associated with them. The following sections provide an overview of the EAF model and a description of the multi-rate MHE framework developed. The performance is thereafter illustrated through application to a case study based on the EAF model.

2. EAF MODEL

The first principles EAF model developed by MacRosty and Swartz (2005) divided the furnace into 4 zones:

(1) the *gas zone*, considers gases in the freeboard volume of the furnace above the scrap material;
(2) the *slag-metal interaction zone*, contains all the slag material and the portion of molten steel zone interacting with it;
(3) the *molten steel zone*, comprises mainly the metals in their liquid state, excluding the portion included in the slag-metal interaction zone; and,
(4) the *solid scrap zone*, represents the solid form of the charged scrap.

Figure 1 is a schematic diagram of the process showing inputs, outputs and material exchanges for the zones. The model equations contain dynamic mass and energy balances, chemical equilibrium, and heat transfer relationships. Chemical equilibrium is considered within the slag and gas zones, and calculated by minimizing the Gibbs free energy. The reactions occurring inside the zones are limited by mass transfer between the zones. Radiation within the furnace and slag foaming are also modeled. Parameter estimation was done using real plant data and verified using additional data sets. The model was re-

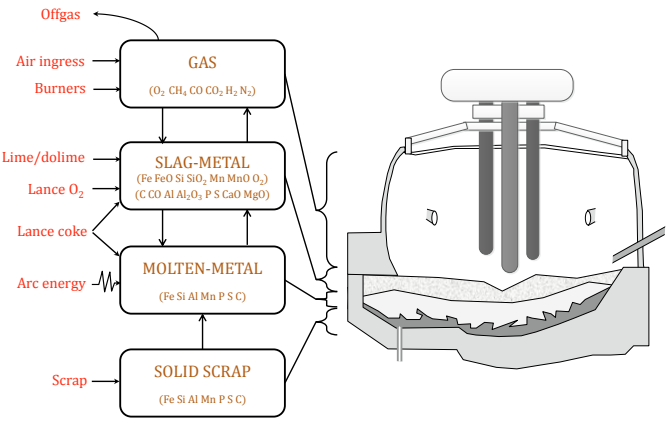

Fig. 1. Schematic of EAF model. (MacRosty and Swartz, 2005)

configured and modified by Sheikhzeinoddin (2011) and Ghobara (2013). The following two major changes were implemented: addition of three JetBoxes which control the supply of oxygen, and assuming a flat surface geometry for scrap melting unlike the cone-frustum assumed by MacRosty and Swartz (2005). The differential-algebraic equation system was modeled in gPROMS and contained 40 differential variables.

This work is built upon the model of Ghobara (2013). The radiation model is removed and replaced with a parameter that divides the energy lost from the arc power through radiation between the roof, the walls, the scrap and the molten metal. Parameter estimation and validation were conducted, with good matching between the model profiles and data obtained. This provided confidence in carrying forward with using such an assumption that removes a lot of nonlinearity in the system. It has been assumed that all the oxides are present in the slag-metal zone, and therefore the oxide states in the molten metal zone were always negligible. Those states were removed from the molten metal, except oxygen which is usually required if lancing occurs. The modified EAF model under consideration has 29 states and flat bath conditions are assumed wherein all the scrap has melted.

3. MOVING HORIZON ESTIMATION

Real-time applications of the EAF model require the states to be known at the time of execution. The state observer needs to estimate the internal states of the EAF system with the limited availability of measurements and various plant-model mismatch scenarios. This would enable the operators to implement effective control strategies during the batch operation. In this section, we present a novel multi-rate MHE framework for EAF operation under flat bath conditions.

The EAF process is very complex to model and there are fluctuations due to frequent addition of materials to the furnace. As with any first principles model, there exists plant-model mismatch and modeling errors. There are also unknown disturbances during the batch operation. The proposed estimation strategy handles the uncertainties though process noise terms. Another issue arises due to the measurements being taken at different sampling rates.

The off-gas compositions viz. the concentration of carbon monoxide (CO), carbon dioxide (CO_2), oxygen (O_2) and hydrogen (H_2), as well as the roof and wall temperatures, are measured every 1 minute. On the other hand, only one sample of slag is taken to determine the composition of iron II oxide (FeO), aluminum oxide (Al_2O_2), silicon dioxide (SiO_2), magnesium oxide (MgO) and calcium oxide (CaO) in the slag. Two sample measurements are usually taken to determine the molten metal temperature and carbon content. The multi-rate nature of the measurements is handled naturally by placing the slow measurements in their proper locations in the measurement history.

3.1 Multi-rate MHE problem formulation

Suppose the EAF model is at time instant t_i where i is the current sampling index and we have a history of past inputs and measurements. The multi-rate MHE includes measurements with various sampling rates. The slower irregular measurements related to slag and molten metal zones can easily be placed in their appropriate locations in the moving horizon frame of length N time intervals. Assuming the slow measurements are positioned at the sampling times of the fast measurements, the vector of fast measurements is defined as $\mathbf{y}_k^F$ and the vector containing both the slow and fast measurements is defined as $\mathbf{y}_k^{SF}$. The measurement distribution can be given as, for example, $\mathbf{Y}_i = \{\mathbf{y}_{i-N}^F, \mathbf{y}_{i-N+1}^{SF}, \mathbf{y}_{i-N+2}^F, \ldots, \mathbf{y}_i^F\}$; where the measurement set at time t_{i-N+1} contains the slow measurements. However, different structures of $\mathbf{Y}_i$ are possible. As time moves forward, when a new measurement becomes available it is appended to the horizon window, and the first measurement is dropped.

Consider the multi-rate MHE problem for a nonlinear system which is observable along the state trajectories in the following general form:

$$\min_{\mathbf{x}_{i-N}, \mathbf{w}_k} \sum_{k=i-N}^{i-1} ||\mathbf{w}_k||^2_{Q^{-1}} + \sum_{\substack{k=i-N \\ k\in\mathbb{I}_F}}^{i} ||\mathbf{y}_k^F - \mathbf{h}^F(\mathbf{x}_k)||^2_{(R^F)^{-1}} + \sum_{\substack{k=i-N \\ k\in\mathbb{I}_{SF}}}^{i} ||\mathbf{y}_k^{SF} - \mathbf{h}^{SF}(\mathbf{x}_k)||^2_{(R^{SF})^{-1}} + ||\mathbf{x}_{i-N} - \hat{\mathbf{x}}_{i-N}||^2_{S_i^{-1}} \quad (1)$$

$$\text{s.t. } \mathbf{x}_{k+1} = \mathbf{f}(\mathbf{x}_k, \mathbf{u}_k) + \mathbf{w}_k, k = i-N, \ldots, i-1 \quad (2)$$

$$\mathbf{x}^{LB} \leq \mathbf{x_k} \leq \mathbf{x}^{UB}, \quad (3)$$

where $\mathbf{x}_k$ is the system state vector, $\mathbf{u}_k$ is the control input, $\mathbf{w}_k$ is a piecewise constant noise term introduced to model the model uncertainty (i.e. the process noise) , $\hat{\mathbf{x}}_{i-N}$ is an estimate for the state at the beginning of the horizon, $\mathbf{f}$ integrates the model, given the state $\mathbf{x}_k$, control input $\mathbf{u}_k$ and process noise $\mathbf{w}_k$, over one sampling interval, and $\{\mathbf{h}^F, \mathbf{h}^{SF}\}$ are the measurement functions that map the system state to $\mathbf{y}_k^F$ and $\mathbf{y}_k^{SF}$ respectively. Q, R^F, R^{SF} and S_i are the covariance matrices (of appropriate dimensions) for the model noise, measurement noise and for the arrival cost respectively. $\mathbf{x}^{LB}$ and $\mathbf{x}^{UB}$ represent lower and upper bounds respectively on the state variables.

The cost function (1) comprises four terms of which the first three are weighted minimization of errors over a time horizon. The fourth term of (1), the arrival cost, summarizes the previous measurement data not considered in the moving horizon frame. The weighing matrix S_i is updated to S_{i+1} for the next MHE run using the solution of the currently solved MHE optimization problem. An EKF update is used in general (Rao et al., 2003),

$$S_{i+1} = Q + A_i[S_i - S_i C_i^T (R + C_i S_i C_i^T)^{-1} C_i S_i] A_i^T \quad (4)$$

where $A_i = \nabla_{\mathbf{x}} \mathbf{f}(\mathbf{x}^*_{i-N}, \mathbf{u}_{i-N}, \mathbf{w}^*_{i-N})$ and $C_i = \nabla_{\mathbf{y}} \mathbf{h}(\mathbf{x}^*_{i-N})$. $\mathbf{x}^*_{i-N}$ and $\mathbf{w}^*_{i-N}$ represent solution of MHE optimization problem (1).

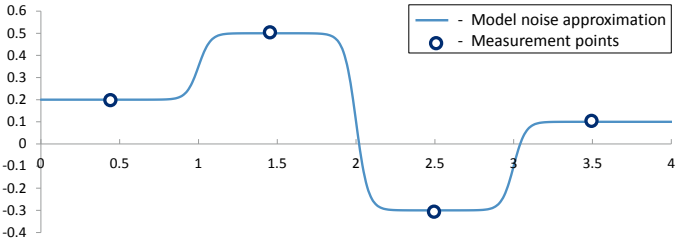

Fig. 2. A continuous, differentiable approximation $W_i'(t, w_k)$ to the piecewise constant process noise function $W_i(t, w_k)$.

3.2 Parameter estimation framework

To transform the multi-rate MHE formulation into a parameter estimation problem, the decision variables of (1) need to be parameters rather than variables. The discrete values of process noise term $\{w_{i-N}, w_{i-N+1}, \ldots w_{i-1}\}$ for a state can be expressed as a discontinuous piecewise constant function $W_i(t, w_k)$. $W_i(t, w_k)$ is replaced by a continuous function $W_i'(t, w_k)$ which treats $\{w_{i-N}, w_{i-N+1}, \ldots w_{i-1}\}$ as parameters. An approximation based on hyperbolic tangent functions is given as (Pantelides, 2015),

$$W_i'(t, w_k) = \frac{1}{2}(w_{i-N} + w_{i-1} + \sum_{k=i-N}^{i-2} (w_{k+1} - w_k) \tanh \frac{\alpha}{\delta t}(t - t_k)), \quad (5)$$

where α is a positive constant that is used to adjust the quality of the approximation, δt is the time interval duration, and t_k is the time boundary between interval k and $k+1$ (i.e. in the case of intervals of equal length $t_k = k\delta t$). A derivation for this expression is given in the Appendix. The division by δt inside the tanh is used for scaling purposes. Now, $W_i'(t, w_k)$ is treated as an artificial measured variable, measured to be 0 at the mid-points of the time intervals. With the approximation for all the process noise terms, the term $\sum_{k=i-N}^{i-1} ||\mathbf{W}_i'(t_{k+\frac{\delta t}{2}}, \mathbf{w}_k)||^2_{Q^{-1}}$ is introduced in the MHE objective function. Figure 2 illustrates the model noise approximation and the measurement points discussed above.

Remark: It is to be noted that with the EKF update (4), S_i is expected to become a dense matrix instead of a diagonal matrix. To implement this in gPROMS, the term 4 of MHE objective function is defined in the gPROMS model itself using a new variable $J(t) = \sqrt{||\mathbf{x}_{i-N} - \hat{\mathbf{x}}_{i-N}||^2_{S^{-1}}}$ and J is treated as a measured variable. We then consider only one measurement of J being 0 at time $t = 0$ and

the standard deviation as 1. This indirectly includes the original arrival cost term in the MHE objective function.

Using the above reformulations we propose the following multi-rate MHE framework for the EAF model in a DAE form,

$$\min_{\mathbf{x0},\mathbf{w}_k} \sum_{k=i-N}^{i-1} ||\mathbf{W}'_i(t_{k+\frac{\delta t}{2}}, \mathbf{w}_k)||^2_{Q^{-1}} + \sum_{\substack{k=i-N \\ k\in\mathbb{I}_F}}^{i} ||\bar{\mathbf{y}}^F_k - \mathbf{y}^F(t_k)||^2_{(R^F)^{-1}} + \sum_{\substack{k=i-N \\ k\in\mathbb{I}_{SF}}}^{i} ||\bar{\mathbf{y}}^{SF}_k - \mathbf{y}^{SF}(t_k)||^2_{(R^{SF})^{-1}} + J(t_{i-N})^2 \quad (6)$$

$$\text{s.t. } \dot{\mathbf{x}}(t) = \mathbf{f}(\mathbf{x}(t), \mathbf{z}(t), \mathbf{y}(t), \mathbf{u}_k) + \mathbf{W}'_i(t, \mathbf{w}_k) \quad (7)$$

$$\mathbf{0} = \mathbf{h}(\mathbf{x}(t), \mathbf{z}(t), \mathbf{y}(t), \mathbf{u}_k), \quad k = i-N, \ldots, i-1 \quad (8)$$

$$\mathbf{W}'_i(t, \mathbf{w}_k) = \frac{1}{2}\left(\mathbf{w}_{i-N} + \mathbf{w}_{i-1} + \sum_{k=i-N}^{i-2} (\mathbf{w}_{k+1} - \mathbf{w}_k) \tanh \frac{\alpha}{\delta t}(t - t_k)\right) \quad (9)$$

$$\mathbf{x_{dy}}(t) = \mathbf{x}(t) - \mathbf{x0}_i \quad (10)$$

$$\mathbf{x_{dy}}(0) = 0 \quad (11)$$

$$J(t) = \sqrt{||\mathbf{x0}_i - \hat{\mathbf{x}}_{i-N}||^2_{S_i^{-1}}} \quad (12)$$

$$\mathbf{x0}_i \in X, \mathbf{w}_{i-N} \ldots \mathbf{w}_{i-1} \in Y \quad (13)$$

where i is the current time index at which the MHE problem is solved, $\mathbf{x0}_i$ is a vector of parameters specifying the initial conditions of the DAE system represented by the $\mathbf{f}$ and $\mathbf{h}$ functions, $J(t)$ represents the arrival cost term, $\{\bar{\mathbf{y}}^F_k, \bar{\mathbf{y}}^{SF}_k\}$ are the measurement vectors, $\mathbf{z}(t)$ are the algebraic variables which are not measured, $\mathbf{y}(t)$ are the measured algebraic variables (both slow and fast) and $\mathbf{x_{dy}}(t)$ are the artificial variables introduced to express the initial conditions of the state variables as parameters $\mathbf{x0}_i$. $\{\mathbf{x0}_i, \mathbf{w}_{i-N}, \ldots, \mathbf{w}_{i-1}\}$ are the parameters to be estimated by the parameter estimation problem. Any constraints on the initial states or the model noise parameters are given by (13). The above multi-rate MHE formulation can be solved using any of the three direct dynamic optimization approaches. It is to be noted that uniform time intervals are used in our application. However, the methodology applies to non-uniform time intervals with a slight modification of notation regarding the interval length.

3.3 Implementation

The multi-rate MHE framework is implemented by using the following software packages: `MATLAB` (MATLAB, 2014), `gPROMS` and `Microsoft Excel`. The modeling and parameter estimation optimization are carried out using `gPROMS/gEST`. The maximum likelihood objective function in the `gPROMS` parameter estimation is reduced to a weighted least squares problem by choosing *constant variance* model for the measured variables. The single shooting approach is used for solving the dynamic optimization problem. The `gPROMS ModelBuilder` (Process Systems Enterprise Ltd., 2015) environment is used to run and represent the model of the process used by MHE. Before each MHE iteration i, the input data required for the model to run are modified in `gPROMS Modelbuilder` manually with the appropriate measurement data, the controls, guesses of the initial states and their respective bounds. The solution of an optimization run is stored in `Microsoft Excel` for plotting.

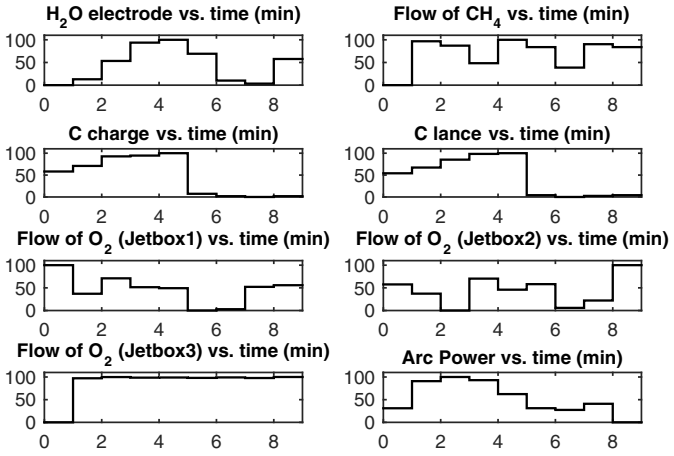

Fig. 3. Normalized nominal input profiles.

The linearization of the model is carried out using `gLINEARIZE` (Process Systems Enterprise Ltd., 2015) to get the A_i and C_i matrices for the arrival cost update (4). Subsequently, the matrix S is updated in an input file by `MATLAB`. The input file is injected into the model using the *Data input Foreign Object* included in `gPROMS 4.1.0`. The hot-starting capability of optimisation-based activities, added to `gPROMS 4.1.0` release, is used to approximate the initial Hessian matrix. A solver option in `gPROMS` enables storage of the Hessian at the termination of an optimization run, which is used in the subsequent run. To reduce the computational time for MHE optimization, the results from the previous MHE run are provided as initial guesses for the next run.

4. CASE STUDY

In this section, the performance of the proposed multi-rate MHE framework for the EAF model is analyzed. We demonstrate the tracking ability of the MHE estimator in the presence of poor initial guesses of the states and a plant-model mismatch. Finally, the computational performance of the strategy is discussed.

The EAF model is considered under flat bath conditions wherein almost all the scrap charge is in molten form. The conditions typically last for the final 20 minutes in a batch of 60 minutes' duration. In this case study, we consider the first 9 minutes out of the full 20 minutes. The measurement values and the *true* states are obtained from a simulation of the original EAF model using a set of nominal inputs represented in fig. 3. Table 1 shows the number of measured variables at different sampling times. The original DAE model is then perturbed with a parametric mismatch to generate a model to be used

Table 1. Multi-rate measurement structure for the case study.

Time (min)	0	1	2	3	4	5	6	7	8	9
Number of measured variables	6	6	6	13	6	6	6	8	6	6

Table 2. State, measurement and model noise covariance values for the case study.

Q	$\text{diag}(36,\ldots,36)$	R^{SF}	$\text{diag}(9,\ldots,9)$
R^F	$\text{diag}(9,\ldots,9)$	S_0	$\text{diag}(16,\ldots,16)$

in the multi-rate MHE framework. The parameter names with their respective mismatches are the power factor (k_p) (+5%), the base mass transfer coefficient (k_m) (−5%) and the oxygen injection factor in the slag-metal zone ($Bias_{O_2}SM$) (+5%). The model equations affected by the mismatch can be found in Ghobara (2013).

An observability test is important before carrying out state estimation. Observability indicates the ability to fully reconstruct the internal states of the system through using the inputs and outputs of the system. For the case study, local linear observability is tested for the nonlinear model by linearizing the model using `gLINEARIZE` at the operating point. The `Obsvf` command in the Control System Toolbox of `MATLAB` is then used to extract the observable states (MATLAB, 2014). By carrying out the above test, the system is found to be fully observable.

The estimator model does not know the exact initial conditions and the initial guesses of the states are generated by perturbing the *true* values by −10%. This scenario is critical, since it reflects what happens in the real plant, where the exact initial conditions are always unknown. The temperatures of the furnace roof and wall, being measured states, are fixed to their measured values. The bounds on the initial states are chosen as ±30% of the *true* values. The parameter α which is used to adjust quality of the model noise approximation is taken as 20. The model noise parameters are bounded as ±1. The values for the MHE covariance matrices (Q, R^{SF} and R^F) as well as the initial value of the arrival cost covariance (S_0) are provided in table 2. The values were determined by trial and error which involved performance analysis of multiple simulations. A moving estimation horizon of 6 minutes and a total estimation horizon of 9 time steps are used. The estimates for a selection of states are compared to the actual plant values in figure 4. For EAF control applications, the molten metal temperature (MM.T) needs to estimated accurately as it determines the tap time which is the time when the molten metal is poured out of the furnace. It is observed that the MHE is showing very good performance in tracking the *true* states and is recovering from erroneous initial states very quickly. Offsets of small magnitudes occurred for a few state variables due to the small total estimation horizon length. However, the corresponding estimated state trajectories show the general trend of convergence towards the *true* profiles.

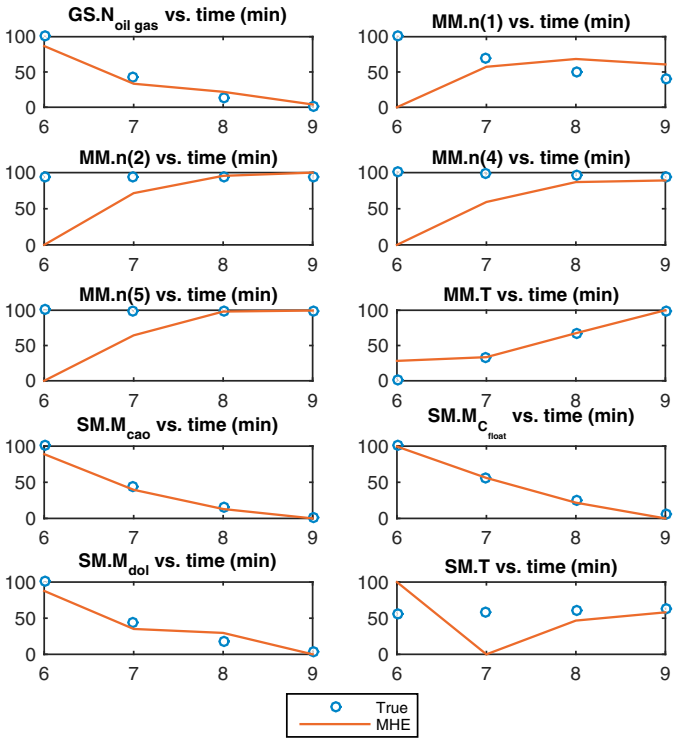

Fig. 4. A selection of normalized state estimates compared with the real trajectory of the states. The MHE tracking ability is demonstrated in the presence of plant-model mismatch and erroneous initial conditions of the states.

4.1 Computational results

The MHE dynamic optimization problem consists of 935 variables and 736 equations. We used an Intel Core i7-3770 processor with 4 CPU cores running Windows at 3.40 GHz to perform the numerical calculations. The solution time history (in CPU seconds) of the 4 MHE runs using the default `gEST` solver tolerances is: 48.2, 70.1, 151 and 51. On average, the MHE problem is solved in 80 CPU seconds. This shows the MHE framework is computationally feasible.

5. CONCLUSION

In this work, we have presented a parameter estimation based multi-rate MHE strategy that is implemented for the EAF operation. The strategy involves approximation of process noise terms with a continuous function. In addition, as MHE considers a past batch of measurements for estimation, both slow and fast measurements typically encountered in an EAF process can be included in a straightforward manner. The state estimation framework developed for the detailed first principles EAF model is suitable for applications related to large scale DAE models. We have used the very-well established sequential strategy for dynamic optimization to solve the multi-rate MHE problem. The estimator showed strong performance in tracking the internal states of the EAF model, in the presence of plant-model mismatch, improving from poor initial guesses of the states.

The short simulation horizon used in the case study is adopted due to the manual implementation of the MHE algorithm. Future work will include automation and evaluation of the estimation framework for the entire duration of the EAF batch under flat bath conditions. Furthermore, we plan to test the proposed multi-rate MHE for cases when the measurements are corrupted with noise. For real time applications of the framework, reducing the MHE solve time will help in the on-line implementation of the model. Finally, an interesting research direction is to explore the effects of increased frequency of slow measurements and quantifying the quality of the state estimates thus obtained.

ACKNOWLEDGEMENTS

The authors would like to acknowledge the comments and suggestions of Dr. C. Pantelides that aided this work. Support from the McMaster Steel Research Centre and the McMaster Advanced Control Consortium is gratefully acknowledged.

REFERENCES

Åkesson, J., Årzén, K.E., Gäfvert, M., Bergdahl, T., and Tummescheit, H. (2010). Modeling and optimization with Optimica and JModelica.org - Languages and tools for solving large-scale dynamic optimization problems. *Computers & Chemical Engineering*, 34(11), 1737–1749.

Allgöwer, F., Badgwell, T.A., Qin, J.S., Rawlings, J.B., and Wright, S.J. (1999). Nonlinear predictive control and moving horizon estimation. An introductory overview. In *Advances in Control*, 391–449. Springer.

Billings, S., Boland, F., and Nicholson, H. (1979). Electric arc furnace modelling and control. *Automatica*, 15(2), 137–148.

Fourer, R., Gay, D.M., and Kernighan, B.W. (1990). A modeling language for mathematical programming. *Management Science*, 36(5), 519–554.

Ghobara, Y. (2013). *Modeling, Optimization and Estimation in Electric Arc Furnace (EAF) Operation*. Master's thesis, McMaster University.

Houska, B., Ferreau, H.J., and Diehl, M. (2011). ACADO toolkit - An open-source framework for automatic control and dynamic optimization. *Optimal Control Applications and Methods*, 32(3), 298–312.

Kraus, T., Kuhl, P., Wirsching, L., Bock, H.G., and Diehl, M. (2006). A moving horizon state estimation algorithm applied to the Tennessee Eastman benchmark process. In *Multisensor Fusion and Integration for Intelligent Systems, 2006 IEEE International Conference on*, 377–382. IEEE.

Lima, F.V. and Rawlings, J.B. (2011). Nonlinear stochastic modeling to improve state estimation in process monitoring and control. *AIChE Journal*, 57(4), 996–1007.

López-Negrete, R. and Biegler, L.T. (2012). A moving horizon estimator for processes with multi-rate measurements: A nonlinear programming sensitivity approach. *Journal of Process Control*, 22(4), 677–688.

MacRosty, R.D. and Swartz, C.L.E. (2005). Dynamic modeling of an industrial electric arc furnace. *Ind.Eng.Chem.Res.*, 44, 8067–8083.

MATLAB (2014). *version 8.4.0 (R2014b)*. The MathWorks Inc., Natick, Massachusetts.

Pantelides, C. (2015). Personal communication.

Process Systems Enterprise Ltd. (2015). gPROMS, www.psenterprise.com/gproms, 1997-2015.

Rao, C.V., Rawlings, J.B., and Mayne, D.Q. (2003). Constrained state estimation for nonlinear discrete-time systems: Stability and moving horizon approximations. *Automatic Control, IEEE Transactions*, 48(2), 246–258.

Sheikhzeinoddin, T. (2011). Modeling, optimization and estimation in electric arc furnace (EAF) operation. In *McMaster Steel Research Centre Meeting*.

Wang, F., Jin, Z., Zhu, Z., and Wang, X. (2005). Application of extended Kalman filter to the modeling of electric arc furnace for power quality issues. In *Neural Networks and Brain, 2005. ICNN&B'05. International Conference on*, volume 2, 991–996. IEEE.

Zavala, V.M. and Biegler, L.T. (2009). Optimization-based strategies for the operation of low-density polyethylene tubular reactors: Moving horizon estimation. *Computers & Chemical Engineering*, 33(1), 379–390.

Appendix A. DERIVATION OF $W_I'(T, W_K)$ BASED ON HYPERBOLIC TANGENT FUNCTIONS

Consider a general hyperbolic tangent function described as $y = f(x) = d + a\tanh b(x - c)$, where x and y are the independent and dependent variables respectively. The constants a and b define the function's amplitude and slope respectively. The constants d and c are used to shift the function curve along the y-axis and x-axis respectively. The function can be considered as a continuous approximation of a discontinuous function given as

$$y' = f'(x) = \begin{cases} d-a & x \in (-\infty, c) \\ d & x = c \\ d+a & x \in (c, \infty) \end{cases}. \tag{A.1}$$

Using the above, the continuous approximation for the first 2 consecutive constant pieces of the discontinuous piecewise constant function $W_i(t, w_k)$ is approximated as

$$W_i'(t, w_{i-N}, w_{i-N+1}) = \frac{w_{i-N} + w_{i-N+1}}{2} + \frac{w_{i-N+1} - w_{i-N}}{2}\tanh b(t - t_{i-N}). \tag{A.2}$$

The above approximation can be extended for the first 3 consecutive pieces as

$$\begin{aligned} W_i'(t, w_{i-N}, w_{i-N+1}, w_{i-N+2}) &= W_i'(t, w_{i-N}, w_{i-N+1}) + \frac{w_{i-N+1} + w_{i-N+2}}{2} \\ &\quad + \frac{w_{i-N+2} - w_{i-N+1}}{2}\tanh b(t - t_{i-N+1}) \\ &\quad - w_{i-N+1}. \end{aligned} \tag{A.3}$$

Extending the above for the full MHE time horizon, we have

$$\begin{aligned} W_i'(t, w_k) = W_i'(t, w_{i-N}, w_{i-N+1}) &+ W_i'(t, w_{i-N+1}, w_{i-N+2}) \\ &+ \cdots + W_i'(t, w_{i-2}, w_{i-1}) - \sum_{k=i-N+1}^{i-2} w_k. \end{aligned} \tag{A.4}$$

Simplifying the above expression and substituting $b = \frac{\alpha}{\delta t}$ gives (5).